ELSEVIER

Contents lists available at ScienceDirect

# Journal of Molecular Liquids

journal homepage: www.elsevier.com/locate/molliq



# Check for updates

# Polymer-Encapsulated ionic liquids as lubricant additives in non-polar oils

Jieming Yan a,b, Filippo Mangolini a,c,\*

- <sup>a</sup> Texas Materials Institute, The University of Texas at Austin, Austin, TX 78712, USA
- <sup>b</sup> Materials Science and Engineering Program, The University of Texas at Austin, Austin, TX 78712, USA
- <sup>c</sup> Walker Department of Mechanical Engineering, The University of Texas at Austin, Austin, TX 78712, USA

## ARTICLE INFO

#### Keywords: Ionic liquids Encapsulation Lubricant additives Boundary lubrication Tribology

#### ABSTRACT

While ionic liquids (ILs) have attracted much attention as potential next-generation lubricant additives, their implementation in oil formulations has been hindered by their limited solubility in hydrocarbon fluids and corrosivity. Here, we encapsulate an oil-insoluble IL that has been studied in lubrication science, namely 1-hexyl-3-methylimidazolium bis(trifluoromethanesulfonyl)imide ([HMIM][TFSI]), within poly(ethylene glycol dimethacrylate-buytl methacrylate copolymer) (poly(EGDM-c-BMA)) microshells using a mini-emulsion polymerization process. The synthesized poly(EGDM-c-BMA)-encapsulated [HMIM][TFSI] microparticles are shown to be dispersible in a non-polar, synthetic oil (i.e., poly- $\alpha$ -olefin). Tribological experiments indicated that the microcapsules act as an additive reservoir that reduces friction by releasing the encapsulated IL at the sliding interface following the mechanical rupture of the polymer shell. X-ray photoelectron spectroscopy (XPS) measurements provided evidence that [HMIM][TFSI] does not tribochemically react on steel surfaces to create a reaction layer, thus suggesting that this IL reduces friction by generating a solid-like, layered structure upon nanoconfinement at sliding asperities, as proposed by previous nanoscale studies. The results of this work do not only provide new insights into the lubrication mechanism of ILs when used as additives in base oils in general, but also establish a new, broadly-applicable framework based on polymer encapsulation for utilizing ILs or other compounds with limited solubility as additives for oil formulations.

#### 1. Introduction

Mineral or synthetic oils are commonly used to lubricate moving mechanical components [1]. To impart new properties or improve existing ones, lubricants are commonly blended with several additives [1]. Among them, surface-active molecules, which prevent contact between sliding surfaces and create a low shear-strength interface by adsorbing on solid surfaces, are commonly employed to reduce wear ("anti-wear additives") and/or friction ("friction modifiers") [1]. In the last three decades, new emission and efficiency standards imposed on automobile engines have called for the development of cleaner and more energy-efficient friction modifiers and anti-wear additives [2,3]. Among them, ionic liquids (ILs), which are salts with melting temperature below 100 °C composed of organic cations and weakly coordinating anions [4], have drawn much attention in tribological studies owing to their unique properties compared to conventional liquid lubricants, such as high thermal stability, low vapor pressure, and the ability to tailor IL formulations from the wide range of possible ion combinations [5–8]. Even though the promising lubricating properties of ILs have widely been recognized, the underpinning lubrication mechanism is still under debate. Nanoscale tribological studies performed using the surface force apparatus (SFA) and the colloidal atomic force microscope (AFM) between smooth surfaces under nanoconfinement in the absence of mechano-chemical reactions [9-14] demonstrated that ILs form confined, layered ionic structures near solid surfaces. These studies also show that the properties of the IL interfacial layers depend on several factors, including the structure of ILs, amount of absorbed water, applied surface potential, and surface chemistry [12.15]. However, these previous studies were conducted at relatively low normal pressures (<100 MPa). In order to investigate the response of ILs under contact pressures closer to those encountered in engineering applications (>500 MPa), recently Li et al. used in situ AFM to evaluate the pressure-dependent lubrication mechanism of phosphonium phosphate ILs (PP-ILs), which have demonstrated promising tribological properties [16,17]. The results obtained using a diamond-like carbon (DLC)-coated silicon AFM tip sliding on steel at an applied pressure up to  $5.5\pm0.3$ GPa indicated that PP-ILs undergo a pressure-induced morphological change to form a lubricious, quasi-solid interfacial layer [16]. This

E-mail address: filippo.mangolini@austin.utexas.edu (F. Mangolini).

 $<sup>^{\</sup>ast}$  Corresponding author.

interfacial layer was found not to be mechanically stable upon increasing the applied normal pressure above  $5.5\pm0.3$  GPa, but despite the progressive removal of the native oxide layer of the steel substrate upon sliding at applied pressures between  $5.5\pm0.3$  GPa and  $7.3\pm0.4$  GPa, a reduction of nanoscale friction was observed, which was shown to be due to the adsorption of phosphate ions on metallic iron surface. This was proposed to lead to the formation of a densely-packed boundary layer able to reduce nanoscale friction [17].

While nanoscale tribological experiments have not shown the occurrence of any shear-induced mechanochemical reaction between PP-ILs and steel surfaces, macroscale tribological studies performed in the boundary-lubrication regime (normal pressure as high as  $\sim 1~\text{GPa}$ ) consistently show evidence of tribochemical reactions between ILs and metallic surfaces [6,7,18-28]. In particular, phosphorus-containing ILs were shown to react on iron surfaces and form phosphate-rich reaction layers (also called tribofilms) [6,25,26], whose chemistry is similar to the one of tribofilms generated by other organo-phosphates widely used as anti-wear additives, such as tricresyl phosphate [29,30]. The discrepancy between nanoscale and macroscale tribological experiments performed in the presence of phosphorus-containing ILs at elevated normal pressure was attributed by Li et al. to differences in contact conditions: while a negligible temperature rise at the contact occurs in AFM tests owing to the low sliding speed of the tip, the high sliding speeds achievable in macroscale experiments can lead to a drastic increase in contact temperature (up to 140 °C), thus enhancing the rate of tribochemical reactions [17].

Despite the extensive investigation that has already been conducted on the promising lubricating properties of ILs, several major challenges have hindered their wider adoption. First, almost all commonly studied ILs have very limited solubility in mineral or synthetic oils. Because of this, early tribological studies were performed using either neat ILs or solutions of polar base oils containing a low concentration of ILs [19]. In 2012, phosphonium-containing ILs with ions that include long alkyl chains were reported as the first oil-miscible class of ILs [6,25]. Since then, several research groups have evaluated the effect of the molecular structure of the ILs on their miscibility in non-polar oils [31–34]. Despite significant advancements over the last few years, the vast majority of ILs reported in the literature are practically immiscible in non-polar hydrocarbon fluids, making their incorporation in modern oil formulations impractical. For example, chelated orthoborates were reported to have excellent lubricating properties, but are immiscible in non-polar hydrocarbons [35,36]. Secondly, ILs often contain halogenated ions, and can thus react with ambient moisture leading to the release of toxic and corrosive hydrogen halides [37,38]. While the tribological properties of several halogen-free IL have already been evaluated [19], the presence of residual halide contaminants from most synthetic precursors of ILs may lead to corrosion of components made of common engineering materials, such as steel or aluminum alloys [24]. In summary, the exploitation of the wide range of ILs currently available in tribological applications requires the development of solutions able to improve IL miscibility and/or dispersal in non-polar oils, while also preventing any detrimental corrosive effects.

Recently, the encapsulation of ILs within organic and inorganic microshells has been proposed as an effecting method for overcoming the kinetics limitation in mass transport originating from the high viscosity and surface tension of ILs [39,40], facilitating the use of ILs in several applications, including carbon capture, separation, and catalysis. However, the encapsulation of oil-insoluble ILs has not been explored so far as an approach for: (a) introducing ILs in hydrocarbon fluids at a concentration higher than their solubility limit; (b) controlling the release of surface-active ILs at sliding interfaces (following the mechanically-induce breakage of the capsule material) to reduce friction and/or wear; and (c) effectively protecting engineering materials from any undesirable corrosive effects of ILs. Here, we encapsulated a class of oil-insoluble ILs whose tribological properties have been evaluate quite 1-hexyl-3-methylimidazolium extensively, namely bis

(trifluoromethanesulfonyl)imide ([HMIM][TFSI]), within poly(ethylene glycol dimethacrylate-buytl methacrylate copolymer) (poly(EGDM-c-BMA)) microshells, and evaluated their stability when dispersed in non-polar fluids. The results of macroscale tribological testing, combined with *ex situ* X-ray photoelectron spectroscopy (XPS) measurements, indicated that the polymer capsules act as an additive reservoir that selectively releases the encapsulated ILs at the contact region via the mechanical rupture of the polymer shell to reduce friction.

#### 2. Materials and methods

### 2.1. Materials

Durasyn 166X poly- $\alpha$ -olefin (PAO-166, Ineos, USA) was used as based oil, while the additive to be encapsulated was 1-hexyl-3-methylimidazolium bis(trifluoromethanesulfonyl)imide ([HMIM][TFSI]) (purity > 98%, Tokyo Chemical Inc., USA). For the preparation of the polymer capsules, ethyl methacrylate (EMA, 99%), butyl methacrylate (BMA, 99%), ethylene glycol dimethacrylate (EGDM), benzoyl peroxide (BPO, 98%), azobisisobutyronitrile (AIBN, 99%), and poly(vinyl alcohol) (PVA, molecular weight distribution: 85–124 KDa) were obtained from Sigma Aldrich.

### 2.2. Preparation of [HMIM][TFSI] IL capsules

The encapsulation of [HMIM][TFSI] within poly(ethylene glycol dimethacrylate-butyl methacrylate) (poly(EGDM-c-BMA)) microcapsules was achieved by mini-emulsion polymerization [41–47]. More specifically, the mini-emulsion method employed in the current work in an extension of the self-assembly of phase-separated polymer (SaPSeP) method [48] first used by Minami *et al.* [49–51]. Briefly, in this method a shell of crosslinked ethylene glycol dimethacrylate (EGDM) and butyl methacrylate (BMA) is formed by the migration of *in-situ* generated polymers to the liquid/liquid interface of the emulsion. The addition of polymethacrylates to the emulsion was reported to significantly enhance the integrity and homogeneity of the capsules [48]. A detailed description of the synthetic procedure is reported below.

First, poly(butyl methacrylate) (PBMA) was prepared by solution polymerization as follows: BMA was first passed through a neutral alumina column to remove polymerization inhibitors. 60 mg of AIBN was added to 15 mg of BMA dissolved in 13 g of toluene, and the solution was stirred at 70  $^{\circ}\text{C}$  for 24 h under a nitrogen atmosphere. The product was purified via recrystallization in methanol and then dried under vacuum.

The encapsulation of [HMIM][TFSI] in poly(EGDM-c-BMA) was performed via the following procedure: 5 mg of benzoyl peroxide (BPO) and 50 mg of PBMA were dissolved in a 1 g mixture of equal masses of EGDM and [HMIM][TFSI]. 10 ml of 0.5% aqueous PVA was added to the IL/monomer mixture and homogenized at 4000 rpm for 5 min. Capsule polymerization was performed in a sealed vial under nitrogen for 24 h at 70 °C while stirred at 300 rpm. The poly(EGDM-c-BMA)-encapsulated [HMIM][TFSI] capsules (referred to as "IL capsules" in the following) were separated via centrifugation and washed three times with distilled water, then dried under vacuum overnight. The emulsion polymerization procedure was repeated without the addition of [HMIM][TFSI] to produce poly(EDGM-c-BMA) microparticles as a control (referred to as "polymer particles" in the following).

## 2.3. Characterization of IL capsules

The morphology and size distribution of the encapsulated IL microcapsules and poly(EDGM-c-BMA) microparticles were determined with scanning electron microscopy (SEM) using a FEI Quanta 650 ESEM. High-resolution micrographs and energy dispersive X-ray (EDX) spectra were collected using a Hitachi S-5500 STEM. Cross sections were prepared by sectioning capsules fixed in conductive resin (Electron

Microscopy Sciences) using a Leica Ultracut ultramicrotome and imaged with a FEI Tecnai transmission electron microscope (TEM). The block face was then imaged with a Zeiss Supra SEM. Optical micrographs were also collected with a Keyence VK X1100 optical profilometer. Capsule suspension stability was evaluated by preparing a 10 wt.% capsules in PAO via sonication, and regular visual observations were made until phase separation was observed.

The IL loading in the polymer microcapsules was estimated using  $^1\mathrm{H}$  nuclear magnetic resonance (NMR) spectroscopy (Agilent MR 500 spectrometer, scanning frequency: 500 MHz). The sample was prepared by crushing 40 mg of IL capsules in 1 ml of acetone- $d_6$ . 27.035 mg (0.25 mM) of anisole (Sigma Aldrich) was then added as an internal reference [52]. The liquid fraction of the IL capsule was then extracted and allowed to settle for 24 h to remove any residual solids. This process was performed under an inert atmosphere to minimize water uptake during sample preparation.

Viscosity measurements on PAO with added encapsulated IL were performed using an ATS NOVA Advanced Research Rheometer, operated in stress-control mode at a constant stress of 20 Pa with a 30 mm plate/plate configuration. Each measured temperature was equilibrated over 60 s, while the integration time for each viscometry measurement was 60 s. A total of 3 measurements were taken at each temperature (points on the chart are the average values, while error bars are the standard deviation).

## 2.4. Tribological testing

Reciprocating ball-on-flat tribological experiments were conducted with a Bruker UMT-2 tribometer at ambient temperature (298  $\pm$  1 K) and in open air with a relative humidity range of 30-50 %. 4 mm diameter balls and flat substrates were made of 52100 steel (McMaster-Carr, USA). The steel substrate were polished to a final root-mean-square roughness of 2.1  $\pm$  0.4 nm (measured by AFM, over a scanned area of 5 x 5 μm<sup>2</sup>) [24]. All tribological experiments were performed under boundary-lubrication conditions (see calculations of the specific film thickness in the Supporting Information), with an applied load of 5 N, corresponding to a mean Hertzian contact pressure of 985 MPa, at a sliding speed of 2 mm/s and with a stroke length of 4 mm. The number of sliding cycles was 900, which resulted in a total sliding distance of 7.2 m and a sliding time of 60 min. Sufficient lubricant was added to fully immerse the contact region. At the end of tribological experiments, the samples were washed with hexane, sonicated in methanol, and stored at<10% relative humidity.

To quantify the wear rate of the 52100 steel discs after tribological experiments, a Keyence VK X1100 optical profilometer was employed. The average specific wear rate (together with the corresponding standard deviation) was computed from the cross-sectional area of the wear track obtained from at least 10 line-scans across the worn region after subtraction of a linear background.

## 2.5. Surface-Analytical measurements

X-ray photoelectron spectroscopy (XPS) measurements were performed on the steel discs after tribological testing. XPS analyses were carried out using a Kratos Axis Ultra DLD XPS with a monochromatic Al Ka X-ray source. The base pressure in the XPS chamber was  $<1 \times 10^{-6}$  Pa. The spectrometer was calibrated according to ISO 15472:2001 with an accuracy of  $\pm$  0.1 eV. The spectra were acquired at an emission angle (EA) was  $0^{\circ}$  and using an incident X-ray beam of 50  $\mu m$  in diameter. High-resolution spectra were collected in constant-analyzer-energy mode with a pass energy of 40 eV and a step size of 0.1 eV (full-width-at-half-maximum of the Ag  $3d_{5/2}$  peak: 0.77 eV), while survey spectra were acquired using a pass energy of 160 eV and a step size of 1 eV. The spectra were processed using CasaXPS (v2.3.16, Casa Software Ltd, UK). The peak binding energies were referred to the aliphatic carbon signal at 285.0 eV. Quantitative analysis of XPS data was performed

using the method described in Ref. [53]. Briefly, once the integrated area was obtained from fitting the original spectra after background subtraction, the quantification was performed using the first-principles method with Powell's equations [54]. The inelastic mean free path was computed using the Gries G1 formula [55].

#### 3. Results and discussion

Fig. 1a displays scanning electron microscopy (SEM) micrographs of poly(EGDM-c-BMA)-encapsulated <code>[HMIM][TFSI]</code> microparticles. The IL-infused capsules exhibit a spherical morphology with a smooth surface. The particle size distribution (Fig. 1b) computed from SEM images was found to be log-normal with a mean diameter of 5.6  $\pm$  0.1  $\mu m$  and standard deviation of 3.3  $\pm$  0.1  $\mu m$ . Poly(EGDM-c-BMA) microparticles obtained using the same synthetic approach but without the addition of <code>[HMIM][TFSI]</code> show a similar morphology (Fig. S.2a in the Supporting Information) and size distribution, but with a slightly lower mean diameter (3.9  $\pm$  0.1  $\mu m$ , Fig. S.2b in the Supporting Information).

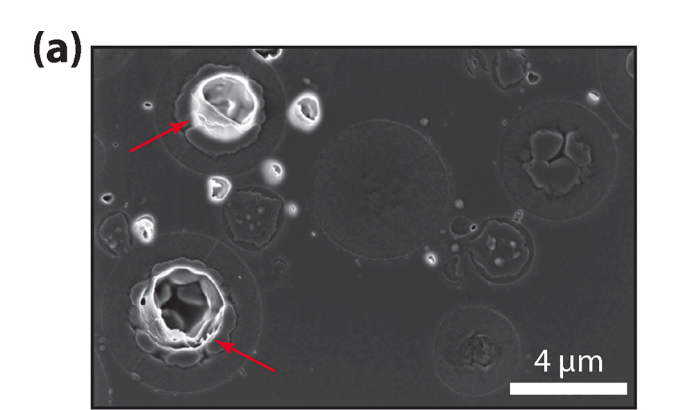
SEM and TEM micrographs of poly(EGDM-c-BMA)-encapsulated [HMIM][TFSI] microparticles embedded in conductive epoxy resin are displayed in Fig. 2. The internal morphology of capsules (see arrows in Fig. 2a) is characterized by the presence of polymeric globules (Fig. 2a) originating from the phase separation of poly(EGDM-c-BMA) at the [HMIM][TFSI]/water interface. The hollow structure of the microparticles (occupied by the IL before the TEM sample preparation) is further apparent in TEM analyses (Fig. 2b), which indicated that the polymer shell thickness is between 0.7  $\mu m$  and 1.2  $\mu m$ . These results are consistent with previous reports using the self-assembly of phase-separated polymer (SaPSeP) method to encapsulate ILs within methacrylate shells [48].

Proton NMR spectroscopic measurements (Fig. S.3 in the Supporting Information) were performed to quantify the IL loading within the capsules. The NMR results indicated that the final [HMIM][TFSI] loading in poly(EGDM-c-BMA) microparticles was approximately 65 wt. %. Additionally, as the analyte was prepared under an inert atmosphere with anhydrous solvents, the water content in the encapsulated [HMIM] [TFSI] could be estimated, and was found to be 0.65 wt.%.

While the IL under investigation in the present work (i.e., [HMIM] [TFSI]) does not exhibit any miscibility in non-polar hydrocarbon fluids and instantaneously undergoes phase separation when added to PAO-166, poly(EGDM-c-BMA)-encapsulated [HMIM][TFSI] could be dispersed in PAO-166. The dispersion (in the current work the maximum concentration of poly(EGDM-c-BMA)-encapsulated [HMIM][TFSI] in PAO-166 was 10 wt.%) was stable for up to 24 h before settling of the ILcontaining capsules owing to the density difference between PAO-166 and the IL capsules (note: redispersing the settled capsules could be easily achieved by agitation), and all oil and capsule mixtures prepared remained homogenous over the course of tribological experiments. The structural and chemical integrity of the capsules was maintained during long-term storage of the encapsulated IL, and no IL leakage from the capsules was observed. Steric stabilization is proposed to be the origin for the particle dispersion stability owing to the solubility of the polymer chains terminating the microshells in PAO-166.

Reciprocating ball-on-disc (52100-vs.-52100 steel) tribological tests were performed at room temperature in the boundary-lubrication regime with neat PAO-166, neat [HMIM][TFSI], and PAO-166 containing different amounts of IL capsules (between 2 wt.% and 10 wt.%). Fig. 3a and 3b displays the evolution of coefficient of friction over time represented by the number of cycles; the number of cycles is plotted in a logarithmic scale in Fig. 3b to highlight the initial (run-in) behavior. In all experiments, the coefficient of friction in the first 5 cycles is 0.13  $\pm$  0.02. However, while in the case of neat PAO-166 and neat [HMIM] [TFSI], the running-in period lasted  $\sim$  10 cycles, the duration of the running-in was found to increase upon increasing the concentration of IL capsules in PAO-166 (Fig. 3b) and approaching the duration of the running-in observed during tests performed with PAO-166 containing

Fig. 1. (a) Scanning electron microscopy (SEM) micrographs of polymer-encapsulated IL (poly(EGDM-c-BMA)-encapsulated [HMIM][TFSI]) deposited on a silicon surface; and (b) size distribution of the microcapsules determined from SEM micrographs.



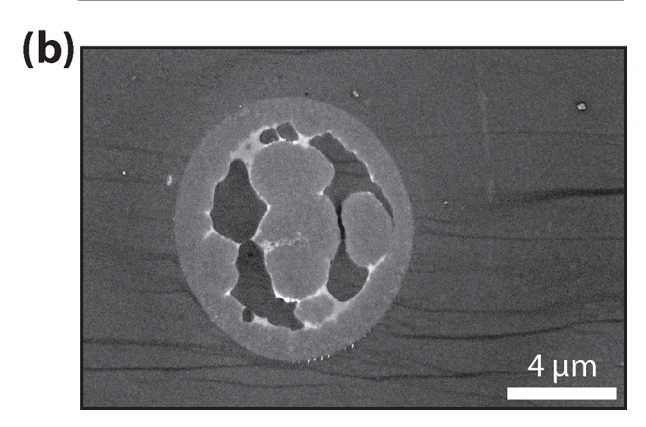


**Fig. 2.** (a) Scanning electron microscopy (SEM) micrographs of polymer-encapsulated IL capsules embedded in conductive resin. The red arrows highlight some of the exposed capsules; and (b) transmission electron microscopy (TEM) micrograph of polymer-encapsulated IL microcapsules showing the hollow structure and the presence of internal polymer globules. (For interpretation of the references to colour in this figure legend, the reader is referred to the web version of this article.)

#### 10 wt.% poly(EGBM-c-BMA) microparticles.

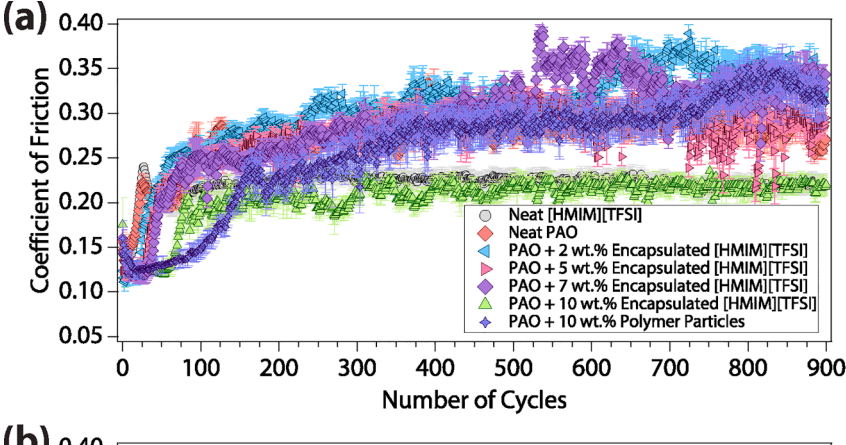
Notably, the steady-state coefficient of friction in the experiments performed with neat [HMIM][TFSI] was significantly lower than the one measured for the tests carried out with neat PAO-166 (Fig. 4a). While no significant decrease in steady-state coefficient of friction was obtained upon introducing the IL capsules to PAO-166 at concentrations between 2 wt.% and 7 wt.%, the 10 wt.% solution of IL capsules in PAO-166 produced a steady-state coefficient of friction similar to the one obtained in tests performed with neat [HMIM][TFSI]. To rule out any potential effect of the poly(EGDM-c-BMA) shell material on the friction response, control experiments were performed with a 10 wt.% solution of polymer particles in PAO-166. The addition of the polymer shell material by itself did not significantly alter the steady-state coefficient of friction when compared to neat PAO-166, thus indicating that the polymeric shell material does not influence the friction response. In

other words, the reduction in steady-state coefficient of friction measured with PAO-166 containing 10 wt.% IL capsules can be directly attributed to the release of [HMIM][TFSI] at the contact interface from a sufficiently high concentration of capsules.

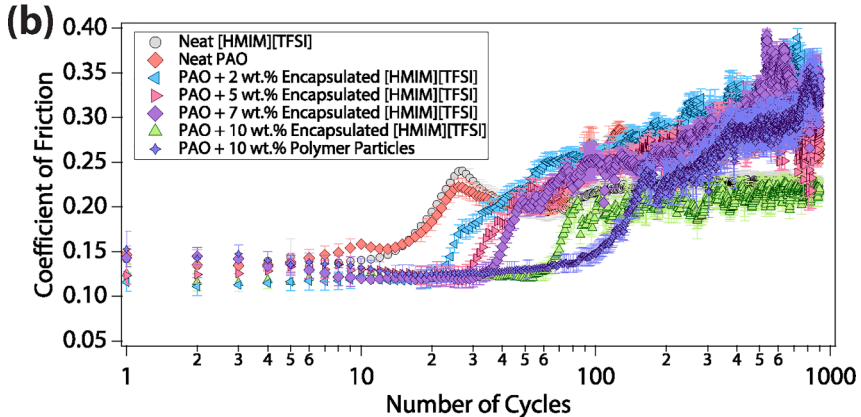
To determine the specific wear rate, optical profilometry measurements were performed on the discs after tribological testing and upon cleaning the worn surface with light solvents (i.e., methanol). The optical microscopy images (Fig. S.4 in the Supporting Information) allowed for the calculation of the specific wear rate (Fig. 4b). While [HMIM][TFSI] was shown to significantly reduce friction, the comparison of the specific wear rate of the specimens used for sliding experiments carried out in neat PAO-166 and neat [HMIM][TFSI] indicated that the IL used in the present work only slightly reduces wear. Additionally, the introduction of either 10 wt.% polymer particles or any concentration of IL capsules results in a similarly small reduction of the specific wear rate, but the degree of wear reduction did not show any dependence on the concentration of IL capsules.

The morphology of the wear tracks generated on the 52100 steel discs indicates a primarily abrasive wear regime. Fig. 5a displays an optical micrograph of a wear track generated during tribological testing with PAO-166 containing 10 wt.% IL capsules. Similar optical micrographs were obtained upon analyzing wear tracks generated during sliding tests carried out with neat PAO-166, PAO-166 containing different concentrations of IL capsules, or PAO-166 with 10 wt.% poly (EGBM-c-BMA) microparticles (without any encapsulated [HMIM] [TFSI]). However, a different wear mechanism was observed in the case of the experiments performed with neat [HMIM][TFSI] (Fig. 5b): the presence of corrosion products in the form of pitting and discoloration in the wear track indicates an abrasive/corrosive wear mechanism, which can be attributed to the reaction between halogenated ILs (such as [HMIM][TFSI]) and adsorbed water (from the atmosphere) in the ILs to form toxic and corrosive hydrogen halides [37,38]. These results indicate that the encapsulation of [HMIM][TFSI] in polymer capsules not only allows for their introduction into non-polar oils, but also limits the IL uptake of water (water is a common contaminant in oils [56]), thus preventing the degradation of the IL due to undesirable side reactions, minimizing corrosion of the contacting metallic surfaces.

While several studies have already demonstrated the promising lubricating properties of ILs [12,13,15], the underpinning lubrication mechanism(s) is still under debate. To gain insights into the interfacial processes that produce the observed reduction in friction and wear, *ex situ* X-ray photoelectron spectroscopy (XPS) analyses were performed. Fig. 6 displays survey XPS spectra acquired in both non-contact and contact (*i.e.*, wear track) regions of 52100 steel disc after tribological testing in the presence of PAO-166 containing 10 wt.% IL capsules. No signals that could be assigned to the presence of physisorbed or chemisorbed [HMIM][TFSI], *i.e.*, fluorine 1 s (F 1 s at 683–688 eV) and sulphur 2p (S 2p at 162–168 eV), were detected both inside and outside the wear track. Similar results were obtained from experiments with different concentrations of IL capsules, or from 10 wt.% polymer particles in PAO-166. These results indicate that under the contact conditions used in the present study, [HMIM][TFSI] does not undergo a shear-



**Fig. 3.** Coefficient of friction as a function of number of cycles obtained during reciprocating ball-on-disc (52100-vs.-52100 steel) tests carried out in neat poly- $\alpha$ -olefin (PAO-166), neat [HMIM][TFSI], PAO-166 containing different weight percentages (from 2 wt.% to 10 wt.%) of IL capsules, and PAO-166 containing 10 wt.% polymer particles. The data are presented with a linear x-axis in (a), while a logarithmic x-axis is used in (b) to highlight the effect of IL capsules on the duration of the running-in period.



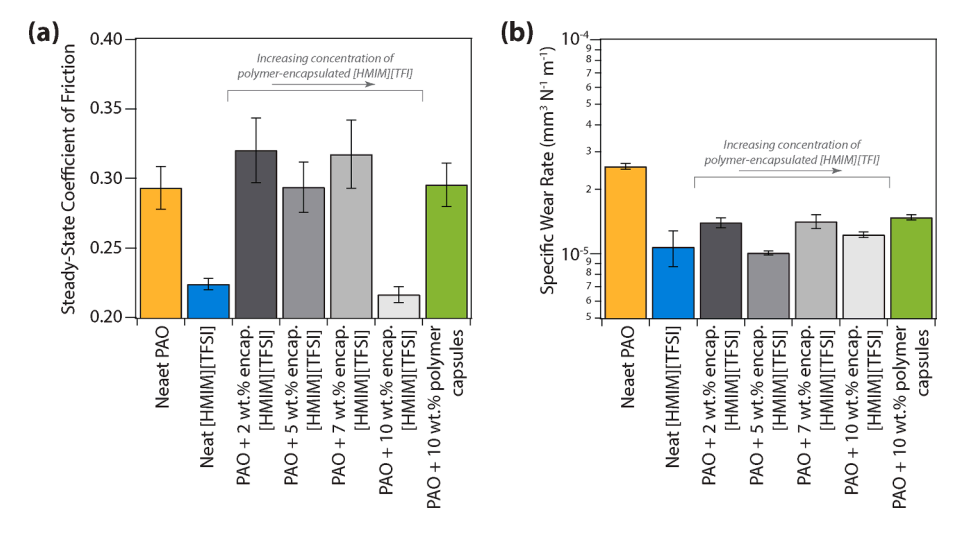


Fig. 4. Steady-state coefficient of friction computed from the last 200 sliding cycles in the data shown in Fig. 3 (a) and specific wear rate (b) measured during reciprocating pin-on-disc (52100-vs.-52100 steel) tests.

induced mechano-chemical reaction with the steel surface to generate a tribofilm. The findings of this study support the conclusions of previous nanoscale tribological experiments that provided evidence for the ability of ILs to undergo a pressure-induced morphological change, which results in the formation of a solid-like interfacial layered structure. This interfacial layer facilitates the sliding of contact surfaces by forming a low shear-strength layer, which is also difficult to squeeze out from the contact region [9–14,16].

While this work provides the first experimental evidence for the potential use of polymer-encapsulated ILs as lubricant additives in non-polar oils, additional studies are necessary to evaluate the mechanical

properties of the polymer capsules and their load-carrying capacity. Our results indicated that the capsules are much larger than the lubricant film thickness (see calculation in the Supporting Information) and thus could not enter the contact. Despite this, the mechanical forces applied to the capsules at the contact inlet are high enough to break the shell (generating polymer fragments in the oil) and release the lubricating phase (i.e., IL).

## 4. Conclusions

Even though ILs have attracted considerable interest in lubrication

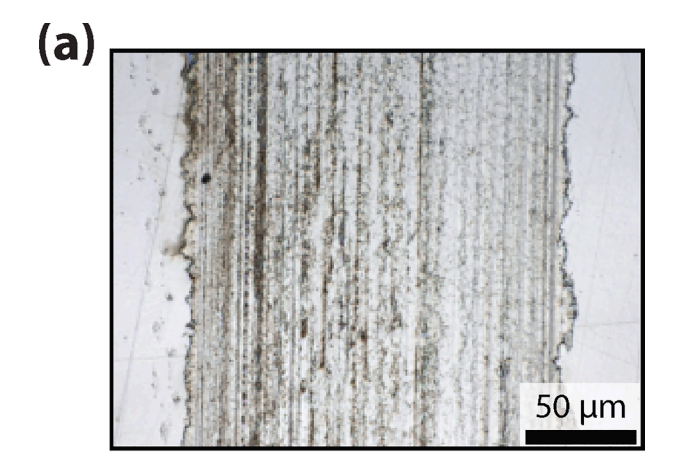




**Fig. 5.** (a) Optical micrograph of a 52100 steel disc after reciprocating ball-ondisc (52100-vs.-52100 steel) tests carried out in PAO-166 containing 10 wt.% of poly(EGBM-c-BMA)-encapsulated [HMIM][TFSI] microcapsules, indicating an abrasive wear mechanism. Similar micrographs were collected on samples used in tribological experiments carried out with neat PAO-166, PAO-166 containing different concentrations of poly(EGDM-c-BMA)-encapsulated [HMIM][TFSI], or PAO-166 with 10 wt.% poly(EGBM-c-BMA) microparticles (without any encapsulated [HMIM][TFSI]); (b) SEM micrograph of 52100 steel disc after reciprocating ball-on-disc (52100-vs.-52100 steel) tests carried out in neat [HMIM][TFSI], indicating an abrasive/corrosive wear mechanism.

science over the last two decades, their implementation in oil formulations has been hampered by their limited solubility in hydrocarbon fluids and corrosivity. Here, we reported a new methodology, based on polymer-encapsulation, for introducing oil-insoluble ILs into non-polar oils. More specifically, we encapsulated an IL that has been extensively studied in tribology, namely 1-hexyl-3-methylimidazolium bis (trifluoromethanesulfonyl)imide [HMIM][TFSI], within poly(ethylene glycol dimethacrylate-buytl methacrylate copolymer) (poly(EGDM-c-BMA)) microshells using a mini-emulsion polymerization process. The synthesized IL capsules have a log-normal size distribution with mean value of 5.6  $\pm$  0.1  $\mu m$  and could be introduced into a synthetic oil (i.e., poly-α-olefin). Tribological experiments indicated that the microcapsules act as an additive reservoir that releases the entrapped IL when needed via the mechanical rupture of the polymer shell at the sliding contact to reduce friction. X-ray photoelectron spectroscopy (XPS) measurements provided new insights into the macroscale lubrication mechanism of [HMIM][TFSI]: the lack of any surface tribochemical reaction of [HMIM][TFSI] on steel to create a reaction layer supports previous nanoscale studies suggesting that ILs reduce friction by undergoing a pressure-induced morphological change to form a solid-like layered structure with low shear strength. The results of this work not only shed new light on the lubrication mechanism of ILs when used as

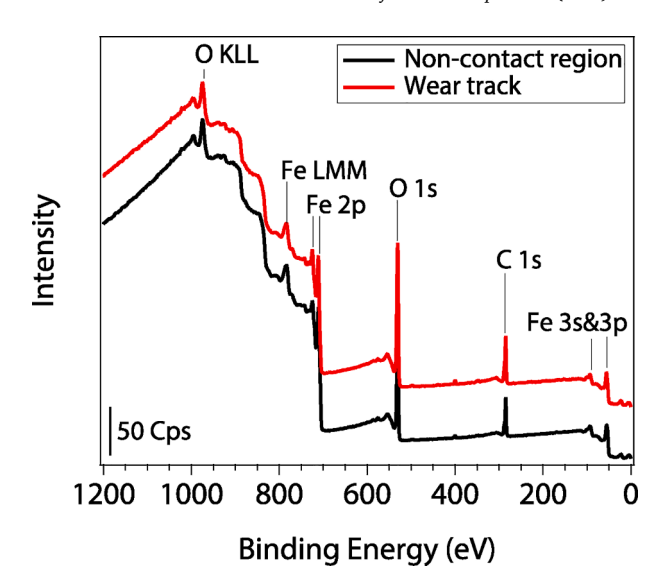


**Fig. 6.** Survey XPS spectra acquired in the non-contact region and inside the wear track of a 52100 steel disc used for tribological testing in the presence of PAO-166 containing 10 wt.% of poly(EGBM-c-BMA)-encapsulated [HMIM] [TFSI] microcapsules.

additives in base oils in general, but also provide a new, broadly-applicable framework based on polymer encapsulation for exploiting ILs or chemical compounds with limited solubility in hydrocarbon fluids as additives for oil formulations.

## CRediT authorship contribution statement

**Jieming Yan:** Conceptualization, Investigation, Data curation, Formal analysis, Writing – original draft, Writing – review & editing. **Filippo Mangolini:** Conceptualization, Investigation, Formal analysis, Writing – original draft, Funding acquisition, Writing – review & editing.

## **Declaration of Competing Interest**

The authors declare that they have no known competing financial interests or personal relationships that could have appeared to influence the work reported in this paper.

## Data availability

Data will be made available on request.

## Acknowledgment

The material is based upon work supported by the Welch Foundation (Grant No. F-2002-20190330) and the National Science Foundation Faculty Early Career Development Program (Grant No. 2042304). F.M. acknowledges support from the 2018 Ralph E. Powe Junior Faculty Enhancement Award sponsored by the Oak Ridge Associated Universities (ORAU), and from the Walker Department of Mechanical Engineering and the Texas Materials Institute at the University of Texas at Austin. The authors thank Dr. Michelle Mikesh for preparing and imaging the capsule cross sections at the Center for Biomedical Research Support Microscopy and Imaging Facility at UT Austin (RRID# SCR\_021756). We would like to thank Dr. Mariam Nouri for the fruitful discussions and laboratory help during the RET program in 2022.

### Appendix A. Supplementary material

Supplementary data to this article can be found online at https://doi.org/10.1016/j.molliq.2023.122089.

#### References

- [1] D.M. Pirro, M. Webster, E. Daschner, Lubrication fundamentals: ExxonMobil, Third edit, CRC Press, Taylor & Francis Group, CRC Press is an imprint of the Taylor & Francis Group, an informa business, Boca Raton, 2016.
- [2] H. Spikes, Low- and zero-sulphated ash, phosphorus and sulphur anti-wear additives for engine oils, Lubr. Sci. 20 (2008) 103–136.
- [3] S.C.C. Tung, M.L.L. McMillan, Automotive tribology overview of current advances and challenges for the future, Tribol. Int. 37 (2004) 517–536, https://doi.org/ 10.1016/j.triboint.2004.01.013.
- [4] D.R. MacFarlane, M. Kar, J.M. Pringle, An Introduction to Ionic Liquids, Fundam. Ion, Liq., Wiley-VCH Verlag GmbH & Co. KGaA, in, 2017, pp. 1–25.
- [5] I. Minami, Ionic liquids in tribology, Molecules 14 (2009) 2286–2305, https://doi. org/10.3390/molecules14062286.
- [6] B. Yu, D.G. Bansal, J. Qu, X. Sun, H. Luo, S. Dai, P.J. Blau, B.G. Bunting, G. Mordukhovich, D.J. Smolenski, Oil-miscible and non-corrosive phosphonium-based ionic liquids as candidate lubricant additives, Wear 289 (2012) 58–64, https://doi.org/10.1016/J.WEAR.2012.04.015.
- [7] J. Qu, J.J. Truhan, S. Dai, H. Luo, P.J. Blau, Ionic liquids with ammonium cations as lubricants or additives, Tribol. Lett. 22 (2006) 207–214, https://doi.org/ 10.1007/s11249-006-9081-0.
- [8] H. Kamimura, T. Kubo, I. Minami, S. Mori, Effect and mechanism of additives for ionic liquids as new lubricants, Tribol. Int. 40 (2007) 620–625, https://doi.org/ 10.1016/j.triboint.2005.11.009.
- [9] S. Perkin, L. Crowhurst, H. Niedermeyer, T. Welton, A.M. Smith, N.N. Gosvami, Self-assembly in the electrical double layer of ionic liquids, Chem Commun. 47 (2011) 6572–6574. https://doi.org/10.1039/C1CC11322D
- [10] O. Werzer, R. Atkin, Interactions of adsorbed poly(ethylene oxide) mushrooms with a bare silica-ionic liquid interface, Phys. Chem. Chem. Phys. 13 (2011) 13479–13485. https://doi.org/10.1039/C1CP20174C.
- [11] R.M. Espinosa-Marzal, A. Arcifa, A. Rossi, N.D.D. Spencer, Microslips to "avalanches" in confined, molecular layers of ionic liquids, J. Phys. Chem. Lett. 5 (2013) 179–184, https://doi.org/10.1021/jz402451v.
- [12] R.M. Espinosa-Marzal, M. Han, A. Arcifa, N.D. Spencer, A. Rossi, Ionic Liquids at Interfaces and Their Tribological Behavior, Ref. Modul. Chem. Mol. Sci. Chem. Eng. (2017), https://doi.org/10.1016/B978-0-12-409547-2.13857-0.
- [13] R. Lhermerout, C. Diederichs, S. Perkin, Are Ionic Liquids Good Boundary Lubricants? A Molecular Perspective, Lubricants. 6 (n.d.). 10.3390/ http://doi.org/10.009
- [14] A.M. Smith, K.R.J. Lovelock, N.N. Gosvami, T. Welton, S. Perkin, Quantized friction across ionic liquid thin films, Phys. Chem. Chem. Phys. 15 (2013) 15317–15320, https://doi.org/10.1039/c3cp52779d.
- [15] Z. Li, F. Mangolini, Recent advances in nanotribology of ionic liquids, Exp. Mech. (2021), https://doi.org/10.1007/s11340-021-00732-7.
- [16] Z. Li, O. Morales-Collazo, R. Chrostowski, J.F. Brennecke, F. Mangolini, In situ nanoscale evaluation of pressure-induced changes in structural morphology of phosphonium phosphate ionic liquid at single-asperity contacts, RSC Adv. 12 (2021) 413–419, https://doi.org/10.1039/d1ra08026a.
- [17] Z. Li, A. Dolocan, O. Morales-Collazo, J.T. Sadowski, H. Celio, R. Chrostowski, J. F. Brennecke, F. Mangolini, Lubrication mechanism of phosphonium phosphate ionic liquid in nanoscale single-asperity sliding contacts, Adv. Mater. Interfaces 7 (2020) 2000426, https://doi.org/10.1002/admi.202000426.
- [18] W. Guo, Y. Zhou, X. Sang, D.N. Leonard, J. Qu, J.D. Poplawsky, Atom probe tomography unveils formation mechanisms of wear-protective tribofilms by ZDDP, ionic liquid, and their combination, ACS Appl Mater. Interfaces 9 (2017) 23152–23163, https://doi.org/10.1021/acsami.7b04719.
- [19] Y. Zhou, J. Qu, Ionic liquids as lubricant additives: a review, ACS Appl. Mater. Interfaces 9 (2017) 3209–3222, https://doi.org/10.1021/acsami.6b12489.
- [20] J. Qu, M. Chi, H.M. Meyer, P.J. Blau, S. Dai, H. Luo, Nanostructure and composition of Tribo-boundary films formed in ionic liquid lubrication, Tribol. Lett. 43 (2011) 205–211, https://doi.org/10.1007/s11249-011-9800-z.
- [21] I. Minami, T. Inada, R. Sasaki, H. Nanao, Tribo-chemistry of phosphonium-derived ionic liquids, Tribol. Lett. 40 (2010) 225–235, https://doi.org/10.1007/s11249-010-9626-0.
- [22] F. Zhou, Y. Liang, W. Liu, Ionic liquid lubricants: designed chemistry for engineering applications, Chem. Soc. Rev. 38 (2009) 2590–2599, https://doi.org/ 10.1039/B817899M.
- [23] L.J. Weng, X.Q. Liu, Y.M. Liang, Q.J. Xue, Effect of tetraalkylphosphonium based ionic liquids as lubricants on the tribological performance of a steel-on-steel system, Tribol. Lett. 26 (2007) 11–17, https://doi.org/10.1007/s11249-006-9175-8.
- [24] Z. Li, H. Celio, A. Dolocan, N. Molina, J. Kershaw, O. Morales-Collazo, J. F. Brennecke, F. Mangolini, Tuning the surface reactivity and tribological performance of phosphonium-based ionic liquid at steel/steel interfaces by bromide/phosphate anion mixtures, Appl. Surf. Sci. (2021), https://doi.org/10.1016/j.apsusc.2021.151245.
- [25] J. Qu, D.G. Bansal, B. Yu, J.Y. Howe, H. Luo, S. Dai, H. Li, P.J. Blau, B.G. Bunting, G. Mordukhovich, D.J. Smolenski, Antiwear performance and mechanism of an oilmiscible ionic liquid as a lubricant additive, ACS Appl. Mater. Interfaces 4 (2012) 997–1002, https://doi.org/10.1021/am201646k.
- [26] J. Qu, H. Luo, M. Chi, C. Ma, P.J. Blau, S. Dai, M.B. Viola, Comparison of an oil-miscible ionic liquid and ZDDP as a lubricant anti-wear additive, Tribol. Int. 71 (2014) 88–97, https://doi.org/10.1016/j.triboint.2013.11.010.
- [27] J. Qu, P.J. Blau, S. Dai, H. Luo, H.M. Meyer, J.J. Truhan, Tribological characteristics of aluminum alloys sliding against steel lubricated by ammonium

- and imidazolium ionic liquids, Wear 267 (2009) 1226–1231, https://doi.org/10.1016/j.wear.2008.12.038.
- [28] Q. Lu, H. Wang, C. Ye, W. Liu, Q. Xue, Room temperature ionic liquid 1-ethyl-3-hexylimidazolium-bis(trifluoromethylsulfonyl)-imide as lubricant for steel-steel contact, Tribol. Int. 37 (n.d.) 547–552. Doi:10.1016/j.triboint.2003.12.003.
- [29] B. Guan, B.A. Pochopien, D.S. Wright, The chemistry, mechanism and function of tricresyl phosphate (TCP) as an anti-wear lubricant additive, Lubr. Sci. 28 (n.d.) 257–265. Doi:10.1002/ls.1327.
- [30] E. Osei-Agyemang, S. Berkebile, A. Martini, Decomposition mechanisms of anti-wear lubricant additive Tricresyl phosphate on iron surfaces using DFT and atomistic thermodynamic studies, Tribol. Lett. 66 (2018), https://doi.org/10.1007/s11249-018-0998-x.
- [31] A.E. Somers, B. Khemchandani, P.C. Howlett, J. Sun, D.R. MacFarlane, M. Forsyth, Ionic liquids as antiwear additives in base oils: influence of structure on miscibility and antiwear performance for steel on aluminum, ACS Appl. Mater. Interfaces 5 (2013) 11544–11553, https://doi.org/10.1021/am4037614.
- [32] A. Khan, S.R. Yasa, R. Gusain, O.P. Khatri, Oil-miscible, halogen-free, and surface-active lauryl sulphate-derived ionic liquids for enhancement of tribological properties, J. Mol. Liq. 318 (2020), 114005, https://doi.org/10.1016/J. MOLLIQ.2020.114005.
- [33] A.E. Somers, R. Yunis, M. Armand, J.M. Pringle, D.R. MacFarlane, M. Forsyth, Towards Phosphorus Free Ionic Liquid Anti-Wear Lubricant Additives, Lubricants. 4 (n.d.). Doi:10.3390/lubricants4020022.
- [34] W.C. Barnhill, H. Luo, H.M. Meyer, C. Ma, M. Chi, B.L. Papke, J. Qu, Tertiary and quaternary ammonium-phosphate ionic liquids as lubricant additives, Tribol. Lett. 63 (2016), https://doi.org/10.1007/s11249-016-0707-6.
- [35] P.K. Khatri, C. Joshi, G.D. Thakre, S.L. Jain, Halogen-free ammonium-organoborate ionic liquids as lubricating additives: the effect of alkyl chain lengths on the tribological performance, New J. Chem. 40 (2016) 5294–5299, https://doi.org/ 10.1039/c5nj02225h.
- [36] F.U. Shah, S. Glavatskih, D.R. MacFarlane, A.E. Somers, M. Forsyth, O. N. Antzutkin, Novel halogen-free chelated orthoborate-phosphonium ionic liquids: synthesis and tribophysical properties, Phys. Chem. Chem. Phys. 13 (2011) 12865–12873, https://doi.org/10.1039/c1cp21139k.
- [37] M.G. Freire, C.M.S.S. Neves, I.M. Marrucho, J.A.P. Coutinho, A.M. Fernandes, Hydrolysis of tetrafluoroborate and hexafluorophosphate counter ions in imidazolium-based ionic liquids, J. Phys. Chem. A. 114 (2010) 3744–3749, https://doi.org/10.1021/jp903292n.
- [38] M. Petkovic, K.R. Seddon, L.P. Rebelo, C. Silva Pereira, Ionic liquids: a pathway to environmental acceptability, Chem. Soc. Rev. 40 (2011) 1383–1403, https://doi. org/10.1039/c004968a.
- [39] Q. Luo, E. Pentzer, Encapsulation of ionic liquids for tailored applications, ACS Appl Mater Interfaces (2019), https://doi.org/10.1021/acsami.9b16546.
- [40] J. Yan, F. Mangolini, Engineering encapsulated ionic liquids for next-generation applications, RSC Adv. 11 (2021) 36273–36288, https://doi.org/10.1039/ dlra05034f.
- [41] T. Dobashi, F.J. Yeh, Q. Ying, K. Ichikawa, B. Chu, an experimental investigation on the structure of microcapsules, Langmuir 11 (1995) 4278–4282, https://doi. org/10.1021/la00011a018.
- [42] K. Ichikawa, Dynamic mechanical properties of polyurethane-urea microcapsules on coated paper, J. Appl. Polym. Sci. 54 (1994) 1321–1327, https://doi.org/ 10.1002/app.1994.070540914.
- [43] H.K. Mahabadi, T.H. Ng, H.S. Tan, Interfacial/free radical polymerization microencapsulation: kinetics of particle formation, J. Microencapsul. 13 (1996) 559–573, https://doi.org/10.3109/02652049609026041.
- [44] Y. Okahata, H. Noguchi, T. Seki, Functional Capsule Membranes. 26. Permeability Control of Polymer-Grafted Capsule Membranes Responding to Ambient pH Changes, Macromolecules. 20 1987 15–21. Doi:10.1021/ma00167a004.
- [45] R. Arshady, Albumin microspheres and microcapsules: methodology of manufacturing techniques, J. Control. Release. 14 (1990) 111–131, https://doi. org/10.1016/0168-3659(90)90149-N.
- [46] R. Arshady, Microspheres and microcapsules, a survey of manufacturing techniques part II: coacervation, Polym. Eng. Sci. 30 (1990) 905–914, https://doi. org/10.1002/pen.760301505.
- [47] A. Loxley, B. Vincent, Preparation of Poly(methylmethacrylate) microcapsules with liquid cores, J. Colloid Interface Sci. 62 (1998) 49–62.
- [48] H. Minami, H. Fukaumi, M. Okubo, T. Suzuki, Preparation of ionic liquidencapsulated polymer particles, Colloid Polym. Sci. 291 (2012) 45–51, https://doi. org/10.1007/s00396-012-2691-1.
- [49] M. Okubo, H. Minami, Formation mechanism of micron-sized monodispersed polymer particles having a hollow structure, Colloid Polym. Sci. 275 (1997) 992–997, https://doi.org/10.1007/s003960050177.
- [50] M. Okubo, Y. Konishi, T. Inohara, H. Minami, Size effect of monomer droplets on the production of hollow polymer particles by suspension polymerization, Colloid Polym. Sci. 281 (2003) 302–307, https://doi.org/10.1007/s00396-002-0774-0.
- [51] H. Minami, M. Okubo, Y. Oshima, Preparation of cured epoxy resin particles having one hollow by polyaddition reaction, Polymer (Guildf). 46 (2005) 1051–1056, https://doi.org/10.1016/j.polymer.2004.11.041.
- [52] C. Li, Z. Su, J. Tan, Y. Xue, Y. Yang, H. Yin, G. Zhang, Q. Zhang, Autocatalyzed interfacial thiol-isocyanate click reactions for microencapsulation of ionic liquids, J. Mater. Sci. 55 (2020) 9119–9128, https://doi.org/10.1007/s10853-020-04670-v.
- [53] F. Mangolini, A. Rossi, N. Spencer, Chemical Reactivity of Triphenyl Phosphorothionate (TPPT) with Iron: An ATR/FT-IR and XPS Investigation, J. Phys. .... (2010) 1339–1354. http://pubs.acs.org/doi/abs/10.1021/jp107617d (accessed October 20, 2013).

- [54] C.J. Powell, The physical basis for quantitative surface analysis by auger electron spectroscopy and X-ray photoelectron spectroscopy, in: N.S. McIntyre (Ed.), Quant, American Society for Testing and Materials, Surf. Anal. Mater., 1978, pp. 5–30.
- [55] S. Tanuma, Electron Attenuation Lengths, in: D. Briggs, J.T. Grant (Eds.), Surf. Anal. by Auger X-Ray Photoelectron Spectrosc., IM Publications, Chichester (UK), n.d.: pp. 259–294.
- [56] P. Parsaeian, A. Ghanbarzadeh, M. Wilson, M.C.P. Van Eijk, I. Nedelcu, D. Dowson, A. Neville, A. Morina, An experimental and analytical study of the effect of water and its tribochemistry on the tribocorrosive wear of boundary lubricated systems with ZDDP-containing oil, Wear 358–359 (2016) 23–31, https://doi.org/10.1016/ j.wear.2016.03.017.